Fluid Phase Equilibria 403 (2015) 49–59

Contents lists available at ScienceDirect

Fluid Phase Equilibria

journal homepage: www.elsevier.com/locate/fluid

Modelling the phase behavior of alkane mixtures in wide ranges of conditions: New parameterization and predictive correlations of binary interactions for the RKPR EOS☆

M. Cismondi Duarte[a,b,*], J. Cruz Doblas[a], M.J. Gomez[a], G.F. Montoya[a]

[a] Phasety, Incubadora de Empresas UNC, Haya de la Torre s/n, Córdoba, Argentina
[b] IDTQ-PLAPIQUI, Universidad Nacional de Córdoba, CONICET, Argentina

ARTICLE INFO

Article history:
Received 21 April 2015
Received in revised form 2 June 2015
Accepted 4 June 2015
Available online 10 June 2015

Keywords:
RKPR
Alkanes
High pressure phase behavior
Critical lines
Hydrocarbons
Interaction parameters correlation

ABSTRACT

After showing in a previous publication a clear superiority to the classic Peng–Robinson EoS for the description of high pressure phase behavior in the more asymmetric alkane–alkane binary mixtures, in this work the RKPR EoS is turned into a predictive model by developing correlations of interaction parameters for all possible pairs or normal alkanes, associated also to a new parameterization of pure compounds. The proposed correlations are based on van der Waals quadratic mixing rules. Repulsive interaction l_{ij} parameters are implemented in all cases, while attractive k_{ij} interactions were necessary only for the methane-series and the more asymmetric systems of propane, in particular with carbon numbers higher than 24. The analysis of the results, in comparison to an important diversity of data available for several dozens of systems, demonstrates a very good predictive power for the new correlations, which could be useful in modeling the phase behavior of different hydrocarbon fluids.

1. Introduction

The alkane–alkane binary systems with higher asymmetry present critical lines extending well beyond 1000 bar at temperatures of interest for the oil industry. These behaviors, specially for the methane-binaries with heavy alkanes, could not be reasonably represented with classic two-parameter equations of state like SRK or PR, not even using both, repulsive and attractive, interaction parameters within quadratic mixing rules [1]. In turn, a very good representation of every system with data available was achieved recently [1] based on the cubic three-parameter RKPR EOS [2] and a new parameterization approach for alkanes.

The modeling of multicomponent mixtures like reservoir fluids requires the availability of interaction parameters for every pair of components present in each particular fluid, at least as a reasonable default matrix from which then some values can be adjusted depending on the case, given that pseudo-components are actually used to describe real fluids (see for example [3]).

The following function is representative of the different k_{ij} values recommended in the literature for methane with higher *n*-alkanes, to be used with the PR EOS (Fig. B1 in Supplementary material).

$$k_{12} = 0.12\left[1 - e^{\left(-\frac{CN_2}{20}\right)}\right] \quad (1)$$

It increases monotonically and tends asymptotically to a maximum of 0.12 for an infinite carbon number in the second compound. Fig. 1 shows the predicted critical lines for several methane + *n*-alkane binary systems, using the PR EOS with k_{ij} values from Eq. (1) and a linear mixing rule ($l_{ij} = 0$) for the co-volume, as it is typical for the modeling of hydrocarbon mixtures in the oil industry. Phase behavior predictions for the first systems in the series are very good, and quite reasonable up to C_{10} approximately. As asymmetry increases, the VLE separations are still correctly predicted within certain low pressure ranges, as it is shown for the mixture with C_{20} in Fig. 2A, but the critical lines are increasingly overpredicted, naturally worsening also the VLE description in the higher pressure ranges. This becomes more pronounced for C_{24} in Fig. 2B.

It becomes clear then that this typical modeling of hydrocarbon mixtures with the SRK or PR equations will have some problems in cases where these asymmetric interactions play an important role, as it is the case with some gas condensate fluids or volatile oils.

☆ Preliminary and/or partial results of this work were presented at the following conferences: 3rd RITeQ (Los Cocos, Argentina, April 13–16, 2014), 27th ESAT (Eindhoven, The Netherlands, July 6–8, 2014)

* Corresponding author.
E-mail address: cismondi@phasety.com (M. Cismondi Duarte).

http://dx.doi.org/10.1016/j.fluid.2015.06.005
0378-3812/

Nomenclature

a_c	Attractive parameter for each fluid in the PR or RKPR EOS
b	Co-volume or repulsive parameter for each fluid in the PR or RKPR EOS
CN	Carbon number of a *n*-alkane
EOS	Equation of state
k_{ij}	Attractive interaction parameter in quadratic mixing rules
l_{ij}	Repulsive interaction parameter in quadratic mixing rules
P_c	Critical pressure
PR	Peng Robinson
RKPR	Generalized Redlich Kwong-Peng Robinson EOS
SRK	Soave Redlich Kwong
T_c	Critical temperature
VLE	Vapor liquid equilibrium
δ_1	Third parameter in the RKPR EOS
ω	Acentric factor

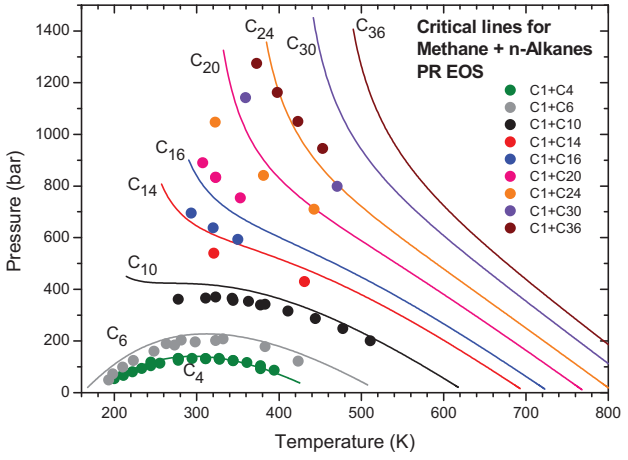

Fig. 1. Typical prediction of critical lines for methane + *n*-alkane binary systems, with the Peng–Robinson EOS. k_{ij} values used in the calculations were obtained from Eq. (1). Experimental data included for comparison (symbols) are the same as in a previous publication [1] where the specific references were given.

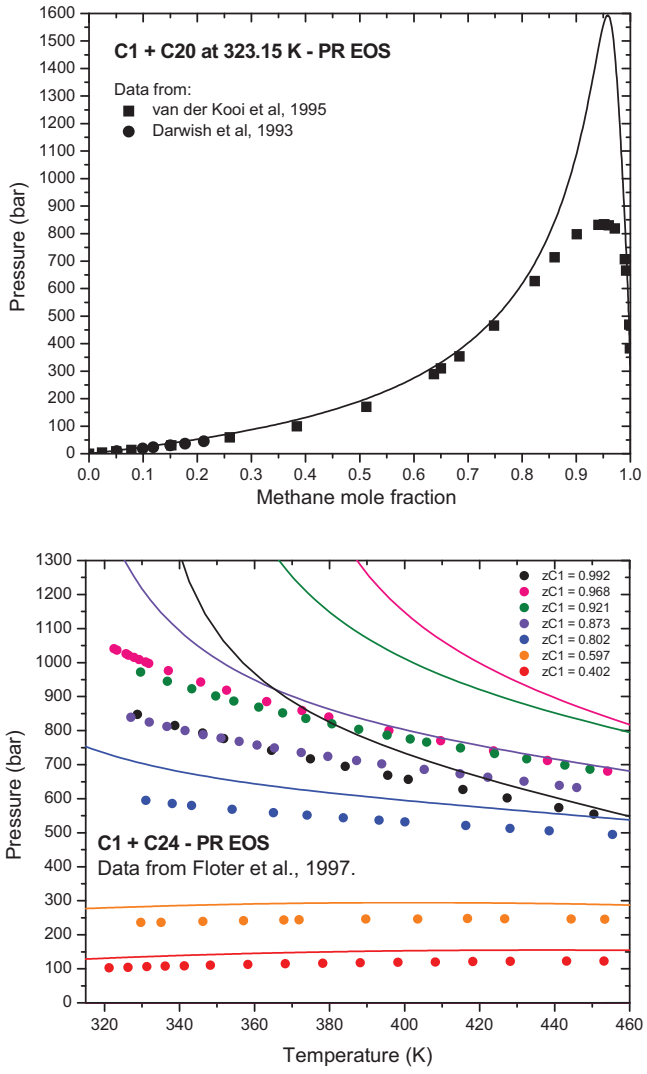

Fig. 2. Illustration of typical prediction of VLE for asymmetric methane + *n*-alkane binary systems, with the Peng–Robinson EOS. (A) Isothermal Pxy diagram for $C_1 + C_{20}$ at 353.15 K. (B) Isopleths for different $C_1 + C_{24}$ mixtures. k_{ij} values used in the calculations (0.0759 and 0.0839, respectively) were obtained from Eq. (1).

Recently, a different and important attempt to use the PR EoS in a predictive way has been the so-called PPR78 [4], based on group contribution temperature dependent k_{ij} values. That work in particular presented very good predictions for not very asymmetric alkane mixtures, and in some cases also for the more asymmetric ones but only in the lower pressure conditions. Nevertheless, a clear and systematic overprediction of bubble pressures can be observed in their Fig. 7 [4] for $C_1 + C_{24}$ until methane mole fractions of at least 0.70, with the predicted curve crossing the experimental data at higher methane concentrations (we encountered the same type of limitation with the PR EoS, illustrated for example for $C_1 + C_{20}$ in Fig. 5 in our previous work [1]). But much more important is what happens for larger carbon numbers. Fig. 11 in the work by Jaubert and Mutelet [4] shows isothermal VLE regions until predicted critical pressures below 500 bar at 373 and 423 K for $C_1 + C_{36}$, while the data by Marteau et al. [5] shows that those regions extend in fact beyond 1200 and 1000 bar, respectively (see Fig. 10 in [1]). It is important to note that the data published by Marteau et al. [5] falls reasonably in trend with data for the other asymmetric methane + *n*-alkane systems (see Fig. 1). Therefore, as it was shown by Jaubert et al. [6], the PPR78 approach allows for very good predictions in multicomponent systems which do not contain those heavier hydrocarbons, but serious limitations could be encountered when such compounds – usually contained in the C_{20} + fraction of reservoir fluids – are present.

Therefore, after having considered the use of the classic two-parameter equations of state, either with constant k_{ij}'s (approach represented by Eq. (1) for methane interactions) or making them temperature-dependent [4], or even including the repulsive l_{ij} interaction [1], it is clear that a different type of model or modeling approach is required to properly capture the phase behavior of the more asymmetric hydrocarbon mixtures.

In this work, based on the promising results in our previous publication [1] and with the goal of developing predictive capacity for the RKPR EOS, correlations of pure compound and interaction parameters are proposed for *n*-alkanes and their mixtures.

Many other articles dealing with the modeling of VLE in *n*-alkanes mixtures using different types of models have been published, and a detailed review is beyond the scope of the present

work. What is remarkable is that in most of those articles the more asymmetric cases have not been covered, or at least not in the higher pressure regions with data available in the literature. A clear proof for such affirmation lies in the relatively low numbers of VLE modeling works citing so far the very important experimental works that have provided data for the more asymmetric systems at high pressures up to close to or more than 1000 bar in the critical region, i.e., van der Kooi et al. [7] for $C_1 + C_{20}$, Flöter et al. [8] for $C_1 + C_{24}$, Machado and de Loos [9] for $C_1 + C_{30}$ and Marteau et al. [5] for $C_1 + C_{36}$. Moreover, it is very difficult to find results comparable to those presented in our previous work [1]. One case is the work by Voutsas et al. [10], where an accurate correlation of the data for the methane mixtures with C_{20}, C_{24} and C_{30} was achieved only with the PC-SAFT EoS with interaction parameters regressed independently for each isotherm. Another similar case, with the simplified PC-SAFT, could be the work by Tihic et al. [11], based on the numbers presented in their Table 5 for C_{20} and C_{30}. Nevertheless, except for our previous work with the RKPR EoS [1], no successful results at all have been found for the correlation of the data from Marteau et al. [5] for $C_1 + C_{36}$, while McCabe et al. [12] have exposed the limitations of its representation with the SAFT-VR EoS.

2. Methodology and results

As a continuation of our previous work [1], essentially the same modeling approach and parameterization strategy were followed here, using the same type of objective functions, but now with the new challenge of developing general correlations for the different series of binary systems instead of individual optimizations. Classic quadratic van der Waals mixing rules were used, considering in principle both, repulsive l_{ij} and attractive k_{ij} interaction parameters. The last one, when used, was made temperature dependent as in the previous work, through the equation

$$k_{ij} = k_{ij}^0 e^{\left(-\frac{T}{T_{c1}}\right)} \tag{2}$$

where T_{c1} is the critical temperature of the more volatile compound. Therefore, there are two parameters that can be adjusted for each system, or rather be correlated for each homologue series as done in this work: l_{ij} and k_{ij}^0.

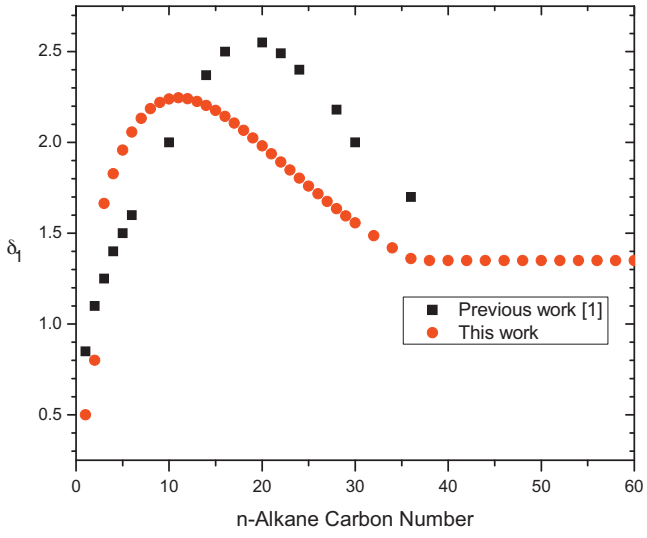

Fig. 3. RKPR third parameter values for *n*-alkanes: the new correlation in comparison to single values published in a previous work [1].

An analysis of the l_{ij} and k_{ij}^0 values, published in the previous work [1] for binaries of methane and ethane with higher alkanes, suggest they could be correlated with the δ_1 parameter of the heavier compound. Along the different optimization stages of this work, such dependency was implemented in different ways for the l_{ij} parameter. In turn, a better correlation for k_{ij}^0 was found in terms of the energetic parameters a_c for the methane series, and also the propane series for the more asymmetric systems (CN > 24). Results were not significantly improved by the use of k_{ij} parameters in the case of ethane and the first part of the propane series, and therefore only l_{ij} was considered in those cases, as also for the higher series, as it will be discussed in detail in the next sections.

It is important to point out that these results correspond to a reparameterization of pure *n*-alkanes, which was performed together with the optimization of interactions for the methane series. Given the evolution of the δ_1 parameter used in the previous work [1], which presents a maximum value to then decrease asymptotically for higher carbon numbers (CN), the following relation was implemented from propane on:

$$\delta_1 = A + B \times \mathrm{CN} \times e^{\left(-\frac{\mathrm{CN}}{\mathrm{CN}^*}\right)} \qquad (3 \le \mathrm{CN} \le 36) \tag{3}$$

obtaining the optimum values $A = 0.91$, $B = 0.33$, $\mathrm{CN}^* = 11$. The values of 0.50 and 0.80 were assigned to C_1 (methane) and C_2 (ethane) while $\delta_1 = 1.35$ was fixed for all *n*-alkanes with CN > 36. The resulting evolution for this third parameter of the RKPR EOS in the normal alkanes family can be appreciated in Fig. 3, where all these values and Eq. (3) are resumed. Table 1 provides numerical values for all the parameters, obtained from matching the critical temperature and pressure, besides the acentric factor, for *n*-alkanes up to C_{60}. The treatment of the heavier *n*-alkanes deserve a separate comment: it is well known that experimental critical constants have been determined with important uncertainties for carbon numbers around 20, and are not available at all or even experimentally accessible for larger numbers [13], which causes that one must resort to a given estimation method or procedure. The chosen method or numbers will of course affect the pure compound parameters, the interaction parameters required in each case and the predictions for mixture properties. During the early stages of this work we explored some possibilities for the heavier compounds until C_{60}, but finally adopted in essence the approach proposed by Schwarz and Nieuwoudt [14], which led us to good results with the propane series, while keeping a regular trend with the DIPPR values available until C_{36} (see Table 1).

All critical lines, critical end points, Pxy diagrams and isopleths presented in the next sections were calculated with either the public or in-house versions of GPEC [15], based on algorithms and calculation methods described elsewhere [16–19].

2.1. The binary series of methane, ethane and propane

The binary systems considered for the correlation of the methane and ethane series were the same as those investigated in the previous work [1] – 9 systems between C_4 and C_{36} for each series – using as well the same selected data for the objective functions. For the propane series, which has not been considered before, 13 systems with available data from the literature were selected between C_4 and C_{60}. The data selected for those systems, to be used in the objective function, are resumed and detailed in Tables A1–A5 in Supplementary material, comprising critical points, biphasic compositions for specified temperature and pressure, and saturation pressures.

The chosen functionality for correlating the l_{ij} parameter in the methane series is given by the equation

Table 1
Pure compound parameters for the RK-PR EOS (This work).[a]

ID	a_c (bar × L^2/mol^2)	b (L/mol)	δ_1	K	T_c (K)	P_c (bar)	ω
C_1	2.3038	0.030434	0.5	1.54085	190.564	45.99	0.01155
C_2	5.6163	0.045611	0.8	1.90384	305.32	48.72	0.09949
C_3	9.8022	0.059875	1.663687	1.95745	369.83	42.48	0.15229
C_4	14.6125	0.076028	1.82759	2.11449	425.12	37.96	0.20016
C_5	20.2237	0.093631	1.957315	2.28763	469.7	33.7	0.251506
C_6	26.4457	0.111805	2.057565	2.45609	507.6	30.25	0.30126
C_7	33.192	0.130552	2.132483	2.62034	540.2	27.4	0.3495
C_8	40.5887	0.150573	2.185714	2.79277	568.7	24.9	0.3996
C_9	48.3293	0.170687	2.220463	2.94352	594.6	22.9	0.4435
C_{10}	56.6611	0.19214	2.239538	3.11287	617.7	21.1	0.49233
C_{11}	65.6307	0.21497	2.245402	3.24457	639	19.5	0.5303
C_{12}	74.543	0.237276	2.240207	3.40514	658	18.2	0.57639
C_{13}	84.9203	0.264005	2.225831	3.54841	675	16.8	0.6174
C_{14}	95.6757	0.290564	2.203908	3.64051	693	15.7	0.64302
C_{15}	105.7858	0.315639	2.175859	3.79189	708	14.8	0.68632
C_{16}	116.4264	0.341676	2.142914	3.90293	723	14	0.7174
C_{17}	125.8201	0.3645	2.106136	4.08196	736	13.4	0.76969
C_{18}	136.4801	0.391618	2.066439	4.22557	747	12.7	0.81136
C_{19}	147.1876	0.418526	2.024609	4.36557	758	12.1	0.85223
C_{20}	157.2669	0.443896	1.981316	4.54638	768	11.6	0.90688
C_{21}	168.285	0.471628	1.93713	4.66597	778	11.1	0.942
C_{22}	179.921	0.501399	1.892534	4.76987	787	10.6	0.97219
C_{23}	190.8514	0.528921	1.847932	4.94285	796	10.2	1.02617
C_{24}	202.2071	0.55802	1.803663	5.08674	804	9.8	1.07102
C_{25}	212.303	0.583397	1.760004	5.19842	812	9.5	1.10526
C_{26}	224.9952	0.616377	1.717185	5.3509	819	9.1	1.15444
C_{27}	235.3702	0.642761	1.675389	5.52846	826	8.83	1.21357
C_{28}	247.5795	0.674698	1.634761	5.60689	832	8.50	1.23752
C_{29}	257.9657	0.701438	1.595415	5.69485	838	8.26	1.26531
C_{30}	269.6807	0.731545	1.557434	5.81961	844	8.00	1.30718
C_{32}	294.1944	0.794773	1.485787	6.02581	855	7.50	1.37655
C_{34}	316.0579	0.850919	1.420068	6.18679	864.8	7.12	1.432
C_{36}	337.0749	0.904344	1.360287	6.44829	874	6.80	1.52596
C_{38}	362.6945	0.970366	1.350	6.57662	882.0	6.42	1.571
C_{40}	387.8337	1.023514	1.350	6.73362	889.6	6.12	1.64
C_{44}	434.2319	1.151222	1.350	7.11557	903.1	5.59	1.780
C_{46}	462.553	1.194387	1.350	7.22773	909.2	5.36	1.849
C_{54}	563.3112	1.422794	1.350	7.84552	929.5	4.60	2.128
C_{60}	639.4866	1.594101	1.350	8.28076	941.8	4.16	2.337

[a] DIPPR values were used for CN up to 32 and 36. For CN = 34 and higher than 36, T_c and P_c were estimated from the correlations by Tsonopoulos and Tan [35], as done previously by Schwarz and Nieuwoudt [14], while the acentric factor was obtained from a linear regression based on the values in Table 10 [14], which in turn implied the use of the method by Magoulas and Tassios [36] for estimation of vapor pressures.

Table 2
Optimized constants for the calculation of l_{ij} values for the three first binary series through Eqs. (4)–(6)

Series	$1000 \times c_L$	$10 \times d_L$	c_{L20}	N_r 20
Methane	6.5463	5.5304	–	–
Ethane	31.470	10.217	0.063733	34.6842
Propane	9.738	3.9258	0.17913	126.676

$$l_{12} = C_L \times \left(1 - e^{\left(\frac{\Delta}{d_L}\right)}\right) \quad ; \quad \Delta = \delta_1(2) - 0.50 \quad 3 \le CN_2$$

(C_1series) (4)

where 2 refers to the less volatile component and CN_2 is its carbon number (3 or higher in this correlation).

For the ethane and propane series the same l_{ij} dependency was initially implemented. But then it was found necessary to use higher values for the more asymmetric systems. In other words, the exclusive dependency with δ_1 (2), which due to Eq. (3) and Fig. 3 would assign the same value to binaries with certain CN larger and lower than 11, was not sufficient for a good correlation of these series. Therefore, a second term depending on CN_2 was added for those systems with $CN_2 > 20$. The resulting expressions are the following:

$$l_{12} = C_L \times \left(1 - e^{\left(\frac{\Delta}{d_L}\right)}\right) \quad ; \quad \Delta = \delta_1(2) - \delta_1(1)$$

(C_2andC_3series : $4 \le CN_2 \le 20$) (5)

$$l_{12} = C_L \times \left(1 - e^{\left(\frac{\Delta}{d_L}\right)}\right) + C_{L20} \times \left(1 - e^{\left(-\frac{CN_2 - 20}{N_r 20}\right)}\right) \quad ;$$

(C_2andC_3series : $CN_2 > 20$) (6)

for which the coefficients are given in Table 2.

The first l_{ij} value in each of the first two series was adjusted independently as $l_{C_1C_2} = -0.0079$and $l_{C_2C_3} = -0.0117$, respectively. The evolution of this interaction parameter along the three series can be seen in Fig. 4A, together with higher series to be discussed in the next section.

In turn, the corresponding final correlations for the k_{ij}^0 parameter in the series of methane and propane, are given by

$$k_{12}^0 = c_K \times \left(1 - e^{\left(\frac{\alpha - 1}{d_K}\right)}\right) \quad ; \quad \alpha = \frac{\alpha_{c2}}{\alpha_{c1}} \qquad CN_2 > 2$$

C_1series (7)

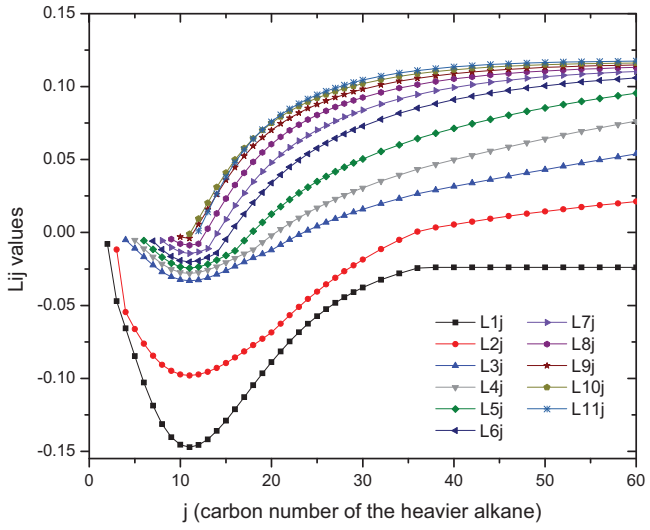

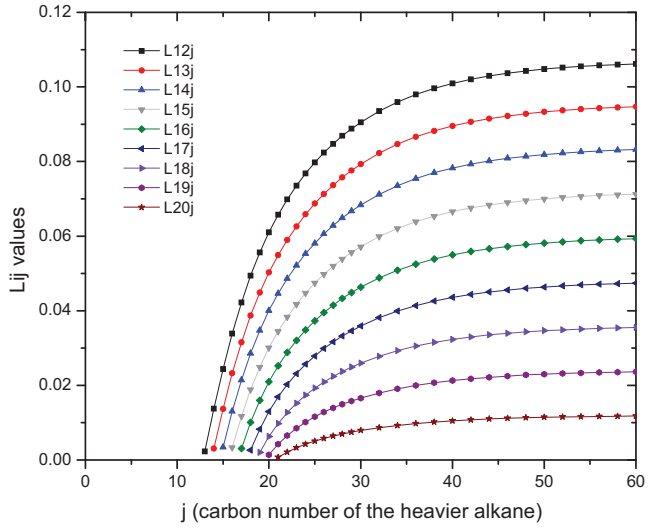

Fig. 4. Evolution of the l_{ij} curves for the different n-alkane + n-alkane binary series. (A) Series from C_1 to C_{11} and (B) series from C_{11} to C_{20}.

Table 3
Optimized constants for the calculation of k^0_{ij} values through Eqs. (7)–(8).

Series	c_K	d_K
Methane—Eq. (7)	0.11027	24.285
Propane—Eq. (8)	−0.15109	5.768

$$k^0_{12} = c_K \times \left(1 - e^{\left(\frac{\alpha-1}{d_K}\right)}\right) \quad ; \quad \alpha = \frac{\alpha_{c2}}{\alpha_{c24}} \qquad CN_2 > 24 \qquad C_3\text{series} \tag{8}$$

$$k^0_{12} = 0 \qquad 2 \le CN_2 \le 24 \qquad C_3\text{series} \tag{9}$$

with the c_K and d_K values given in Table 3. As done for the corresponding l_{ij}, the first interaction in the methane series was independently adjusted to

$$k^0_{C_1C_2} = 0.00307 \tag{10}$$

The values given by Eqs. (7)–(10) together with the constants in Table 3 are graphically condensed in Fig. 5. It is important to note that no k_{ij}'s are used in the proposed correlations for any other binary series between alkanes, i.e., any pair not including methane or propane.

Given the traditional use of a linear mixing rule for the co-volume with classic cubic equations of state like SRK and PR, it could be found surprising the essential role that the repulsive l_{ij} interaction parameter plays in the predictive correlations proposed in this work, while most k_{ij} between alkanes are set to zero. Nevertheless, if thought from a physical or molecular perspective and specifically for n-alkanes mixtures, this is the way it should be. There are no reasons for expecting the stronger or weaker attractions that would be implied by non zero k_{ij} values, between non polar chains of the same type that only differ in length. Instead, the mixing of molecules with different sizes and shapes may well introduce steric or volumetric effects that could be accounted for in

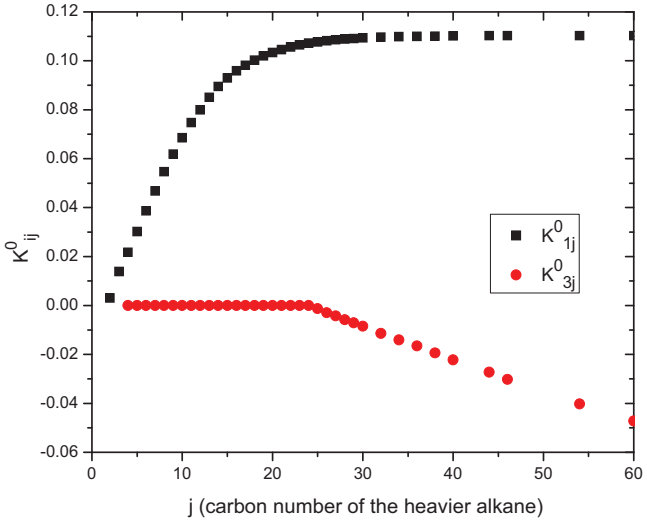

Fig. 5. Evolution of the k^0_{ij} curves, which were defined with nonzero values only for the methane and propane series.

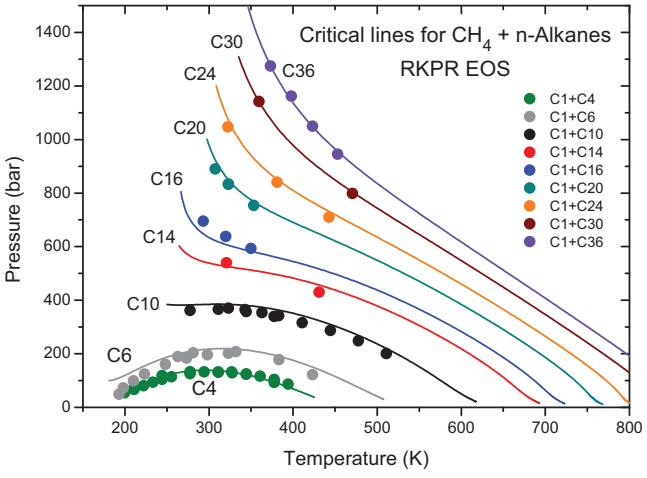

Fig. 6. Prediction of critical lines for different methane + n-alkane binary systems, with the RKPR EOS and correlations developed in this work. Experimental data included for comparison (symbols) are the same as in a previous publication [1] where the specific references were given.

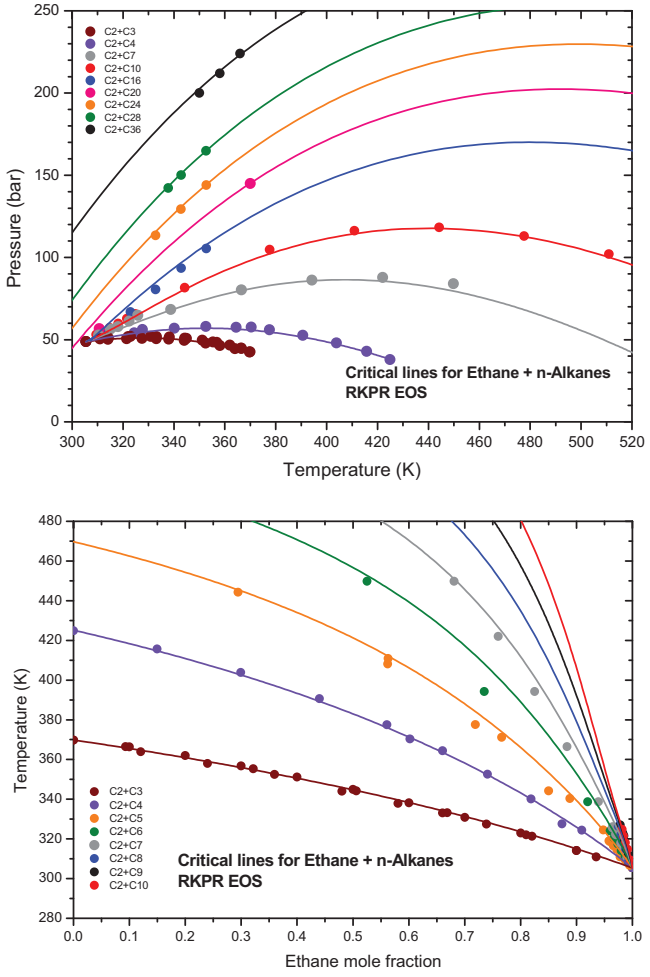

Fig. 7. Prediction of critical lines for different ethane + *n*-alkane binary systems, with the RKPR EOS and correlations developed in this work. Experimental data included for comparison (symbols) are the same as in a previous publication [1] where the specific references were given.

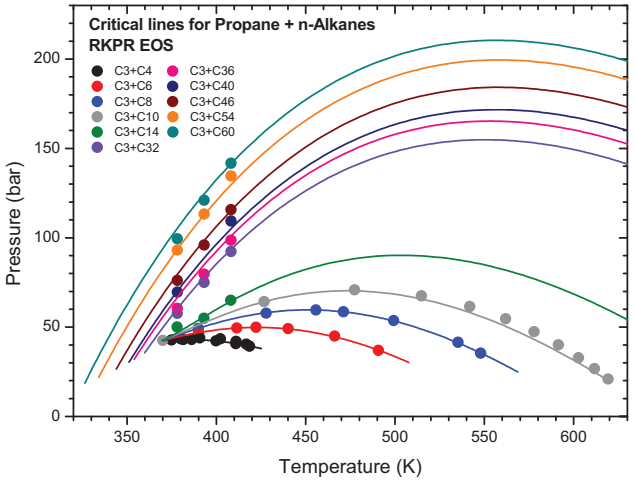

Fig. 8. Prediction of critical lines for different propane + *n*-alkane binary systems, with the RKPR EOS and correlations developed in this work. References for experimental data (symbols) are those given in Table A2 in the Supplementary material.

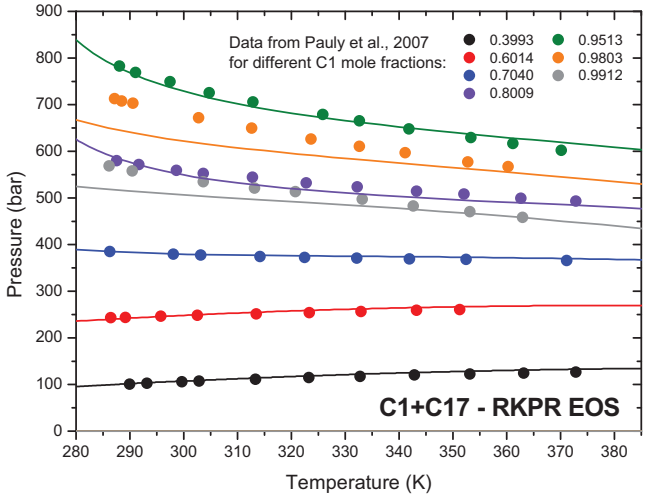

Fig. 9. Prediction of isopleths for different $C_1 + C_{17}$ mixtures, with the RKPR EOS and correlations developed in this work. The data from Pauly et al. [20] were included in order to evaluate the predictions, but not a single data point for this system was used for the adjustment of correlations.

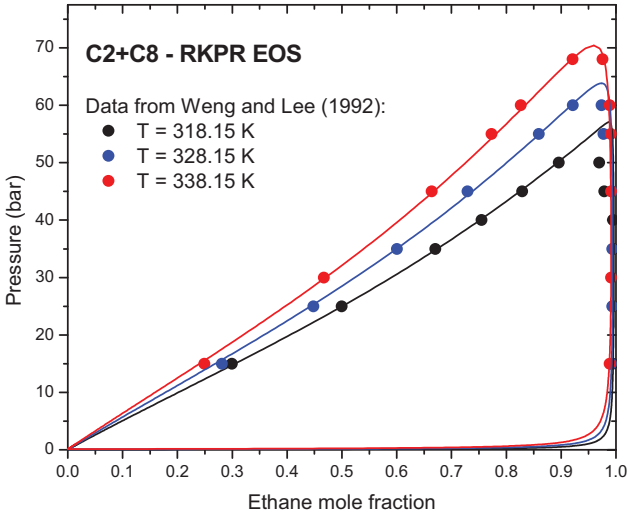

Fig. 10. Prediction of isothermal Pxy diagrams for the system $C_2 + C_8$, with the RKPR EOS and correlations developed in this work. The data from Weng and Lee [21] were included in order to evaluate the predictions, but not a single data point for this system was used for the adjustment of correlations.

the model through the use of non zero l_{ij}'s. Moreover, as previously suggested [1], the third parameter in the RKPR EoS can be interpreted in relation with the effective non-sphericity of the molecule. Then, it appears reasonable to have the l_{ij} parameter correlated with the δ_1 difference, as expressed by Eqs. (4)–(6).

Figs. 6–8 show the predicted critical lines, together with available experimental data for the methane, ethane and propane series of binary systems, respectively. The quality achieved in the predictions with the RKPR EOS and the correlations proposed in this work appears to be excellent, specially if the methane series (the more challenging one, due to the extreme asymmetry with the larger alkanes) is compared to the predictions by the PR EOS in Fig. 1. Predictions of critical lines are very good not only in pressure–temperature, but also in the temperature-composition space, as it is shown in Fig. 7 for the ethane-series.

The predictions of subcritical VLE for different methane + *n*-alkane binaries agree very well with experimental data and results are very similar to those exposed in our previous publication [1]. As

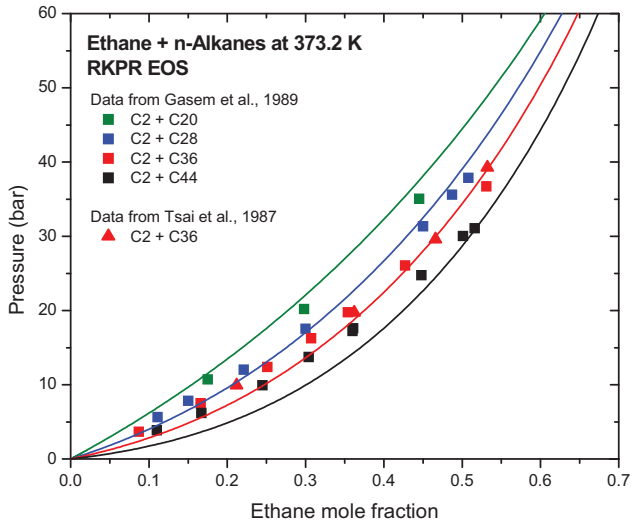

Fig. 11. Prediction of bubble point curves for different C_2 + heavy *n*-alkane systems at 373.2 K, with the RKPR EOS and correlations developed in this work. Experimental data from [22,23].

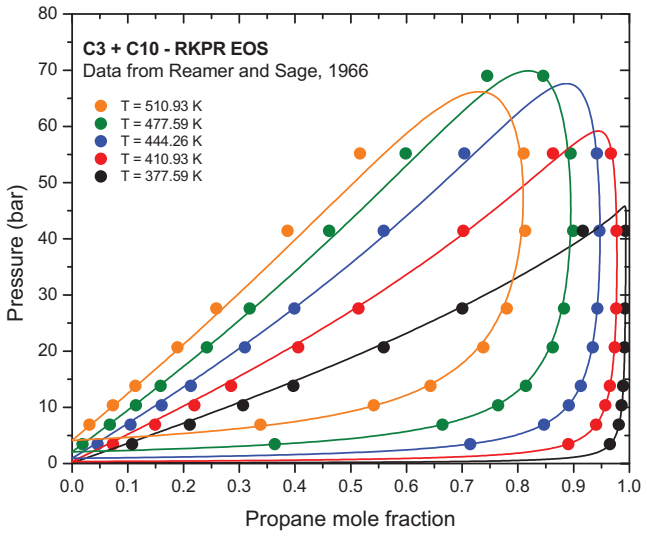

Fig. 13. Prediction of isothermal Pxy diagrams for the system $C_3 + C_{10}$, with the RKPR EOS and correlations developed in this work. Experimental data from [27].

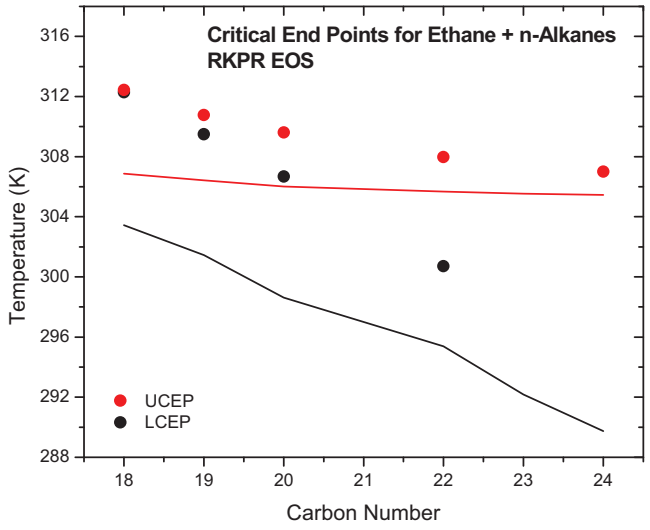

Fig. 12. Prediction of lower and upper critical end point temperatures for C_2 + *n*-alkane systems, with the RKPR EOS and correlations developed in this work. Experimental data from [24,25].

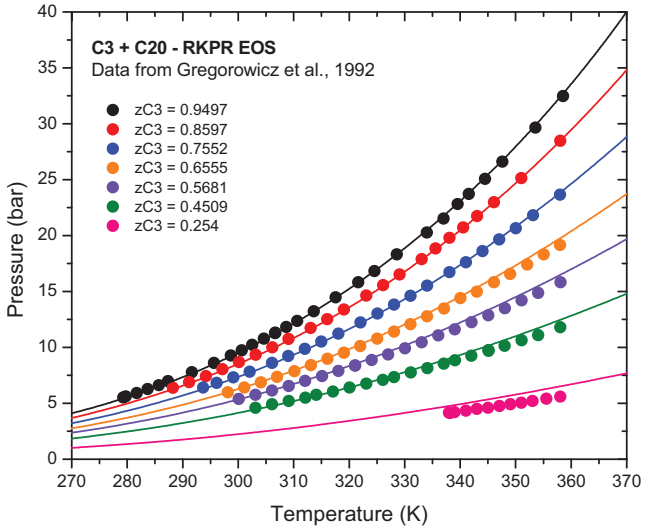

Fig. 14. Prediction of isopleths for different $C_3 + C_{20}$ mixtures, with the RKPR EOS and correlations developed in this work. Experimental data from [28].

a new and different type of result in the sense of being purely predictive since no data of this system was used in the parameterization process, predicted isopleths for different mixtures of $C_1 + C_{17}$ are presented in Fig. 9 showing a very good agreement with experimental data. An equivalent purely predictive result in the ethane-series is presented in Fig. 10 for $C_2 + C_8$, with predictions for VLE at three different temperatures, showing excellent agreement with experimental data.

The prediction of bubble point curves, or in other words solubilities of ethane in different heavy *n*-alkanes from C_{20} to C_{44} at 373.2 K, is presented in Fig. 11. The qualitative trend for the effect of the chain length is correctly predicted and a good quantitative agreement can also be observed.

The prediction of critical end points (CEP's) for the ethane-series is presented in Fig. 12. The evolution of the phase behavior in this series, as well as the qualitative trends for the CEP temperatures with the carbon number of the second alkane, is correctly predicted. Although both the LCEP and UCEP temperatures are systematically overpredicted (which is typical in the use of equations of state without a crossover treatment) the errors are of just a few Kelvin degrees, between 2 and 8.

As an illustration of the predictive capacity of the new developed parameters correlations for the propane series, a very good representation of the phase behavior for the binary systems with *n*-decane and *n*-eicosane can be observed in the form of different isothermal Pxy diagrams and isopleths, in Figs. 13 and 14, respectively. Regarding more asymmetric propane mixtures, Schwarz and Nieuwoudt [14,26] published high pressure saturation points, in particular in the near critical regions, for binary systems of propane with several different heavy *n*-alkanes at three different temperatures. Predictions for the systems with C_{32}, C_{38}, C_{44} and C_{54}, are presented in Fig. 15.

Finally, the most asymmetric system with an important amount and quality of data available in this series is considered in Fig. 16, where predictions for different isopleths of $C_3 + C_{60}$ mixtures are compared with the data from Peters et al. [29]. For other less asymmetric and less challenging propane systems, excellent predictions are also shown in Figs. B2–B8 in Supplementary material.

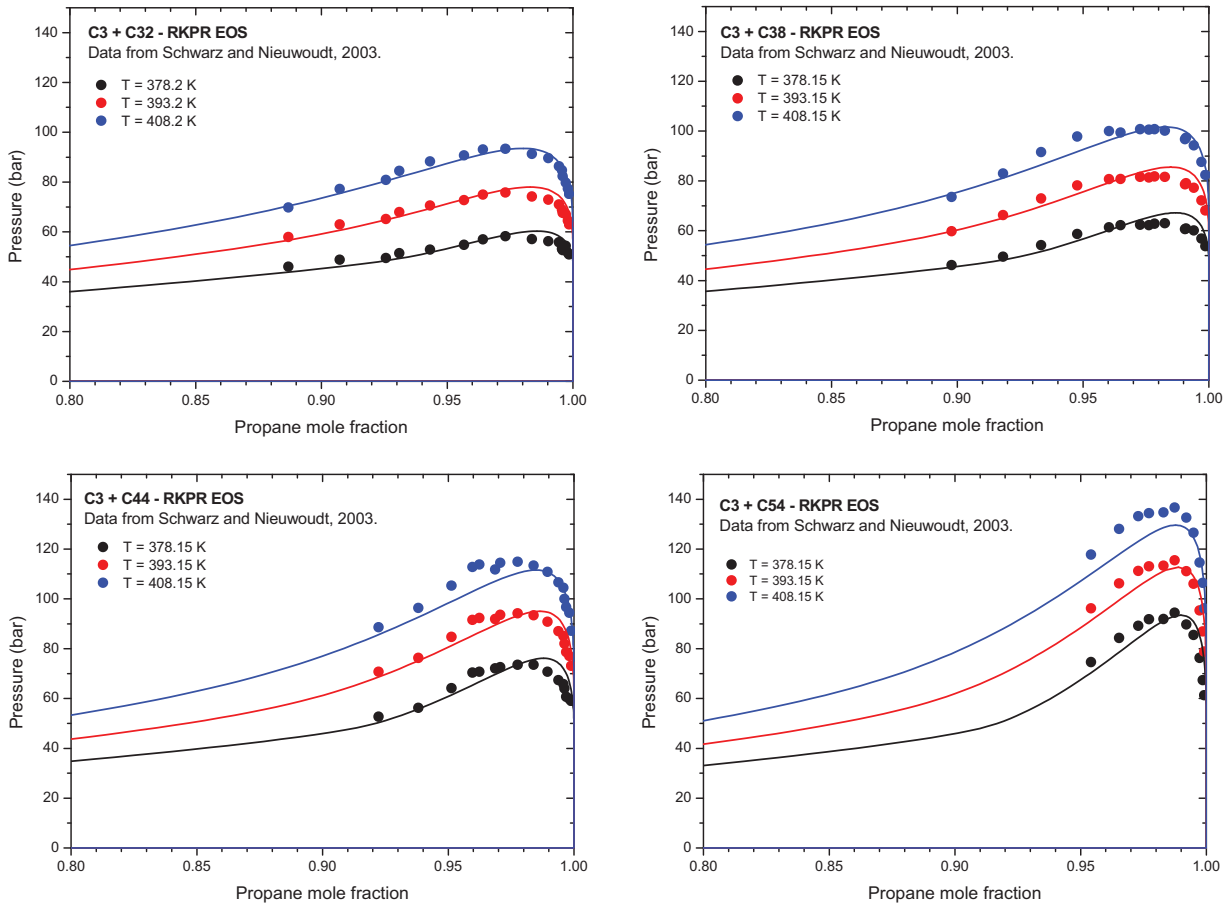

Fig. 15. Prediction of isothermal Pxy diagrams in the critical region for the binary systems of C_3 with C_{32}, C_{38}, C_{44} and C_{54}, with the RKPR EOS and correlations developed in this work. Experimental data from [14,26].

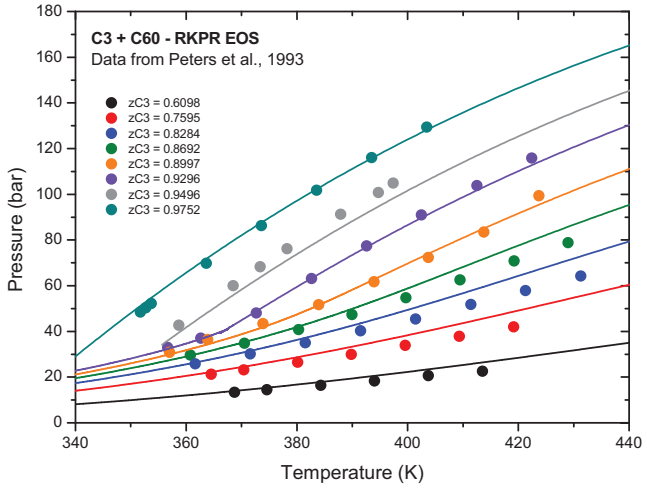

Fig. 16. Prediction of Isopleths for different $C_3 + C_{60}$ mixtures, with the RKPR EOS and correlations developed in this work. Experimental data from [29].

2.2. The binary series of higher n-alkanes

The amount of the data available for the higher series of binary systems between *n*-alkanes is much lower than for the first three series considered in the previous section, and does not allow for the same type of treatment or parameterization strategy. These higher series are clearly not as important as the first ones for the simulation of reservoir or petroleum fluids. Still, they of course play a role and deserve a reasonable treatment in this new parameterization of the RKPR EOS as a predictive model for both synthetic hydrocarbon and real reservoir fluids. Based on the results and the trends identified for the first three series, the expectations were that the implementation of only the repulsive l_{ij} parameter, correlated with the δ_1 parameter through some functionality like Eqs. (5)–(6) should be enough to obtain a good description of the phase behavior as known from experimental data for some mixtures of mainly C_4 and C_6 with higher *n*-alkanes. It was also expected that the l_{ij} curves should then decrease their

Table 4
Constants for the calculation of l_{ij} values through Eqs. (11)–(12).

Series	$1000 \times c_L$	$10 \times d_L$	J	c_{Lj}	N_{rj}
4	11	3.3	18	0.135	60
5	12	2.6	16	0.11	30
6	13	2.0	14	0.10	17
7	14	1.6	13	0.10	14
8	15	1.3	12	0.10	12
9	16	1.1	11	0.10	11
10	17	1.0	11	0.10	10
11	18	0.9	12	0.10	9
12	17	1.0	13	0.09	10
13	15.5	1.0	14	0.08	10
14	14	1.0	15	0.07	10
15	12	1.0	16	0.06	10
16	10	1.0	17	0.05	10
17	8	1.0	18	0.04	10
18	6	1.0	19	0.03	10
19	4	1.0	20	0.02	10
20	2	1.0	21	0.01	10

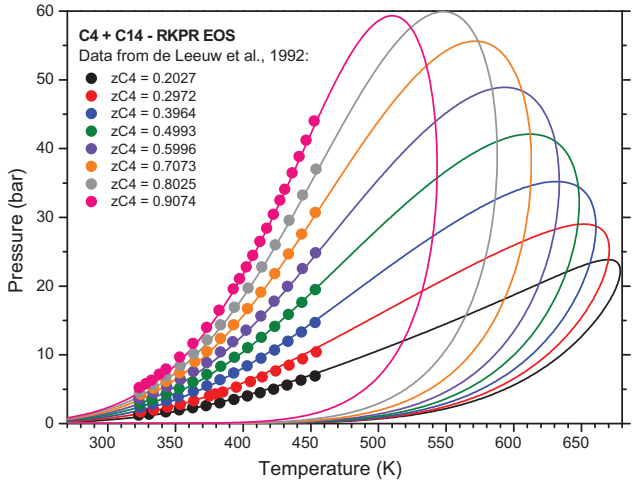

Fig. 17. Prediction of Isopleths for different $C_4 + C_{14}$ mixtures, with the RKPR EOS and correlations developed in this work. Experimental data from [30].

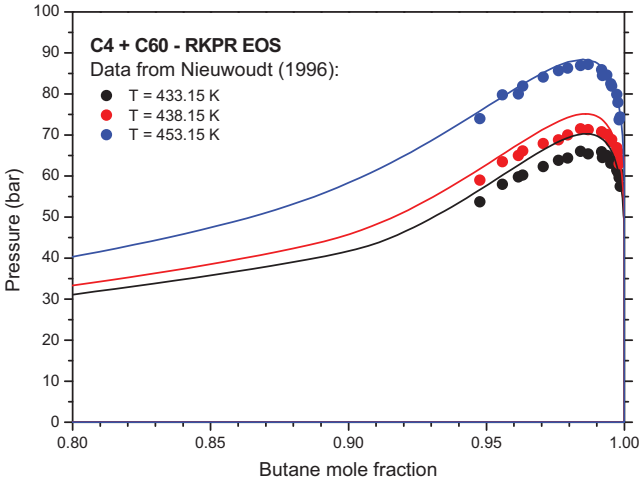

Fig. 18. Prediction of isothermal Pxy diagrams in the critical region for the binary system $C_4 + C_{60}$, with the RKPR EOS and correlations developed in this work. Experimental data from [31].

magnitudes and vanish at a certain point as we go to larger alkanes in the place of the "more volatile" compound. Such behavior is indeed seen in Fig. 4A and B, with the curves resulting from Eqs. (11)–(12) (in fact, a generalization of Eqs. (5)–(6)) and the constants in Table 4.

$$l_{12} = C_L \times \left(1 - e^{\left(\frac{\Delta}{d_L}\right)}\right) \quad ; \quad \Delta = \delta_1(2) - \delta_1(1)$$

$$(C_4 \text{to} C_{20} \text{series} : CN_1 < CN_2 \leq j) \tag{11}$$

$$l_{12} = C_L \times \left(1 - e^{\left(\frac{\Delta}{d_L}\right)}\right) + C_{Lj} \times \left(1 - e^{\left(-\frac{CN_2 - j}{N_{rj}}\right)}\right) \quad ;$$

$$(C_4 \text{to} C_{20} \text{series} : CN_2 > j) \tag{12}$$

Predictions for the system $C_4 + C_{14}$ are compared to the isoplethic sets published by de Leeuw et al. [30] in Fig. 17. For the most extreme asymmetric system of *n*-butane investigated, $C_4 + C_{60}$, predictions are compared with the saturation points in the

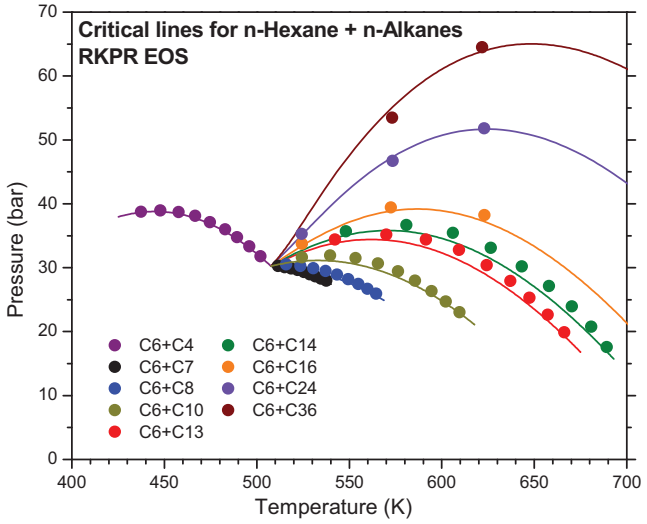

Fig. 19. Prediction of critical lines for different *n*-hexane + *n*-alkane binary systems, with the RKPR EOS and correlations developed in this work. Experimental data from [32–34].

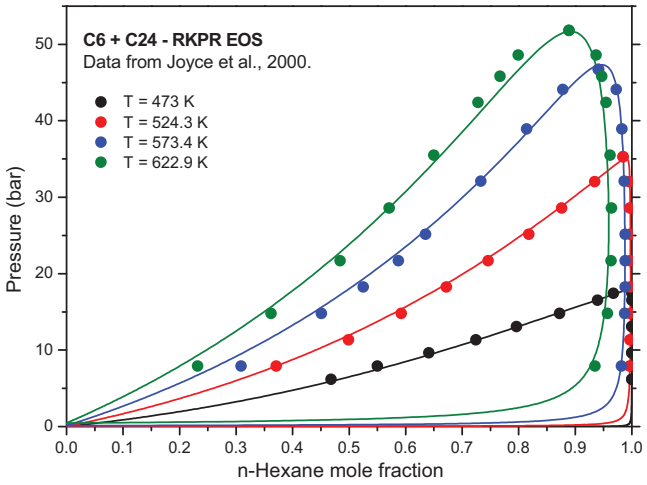

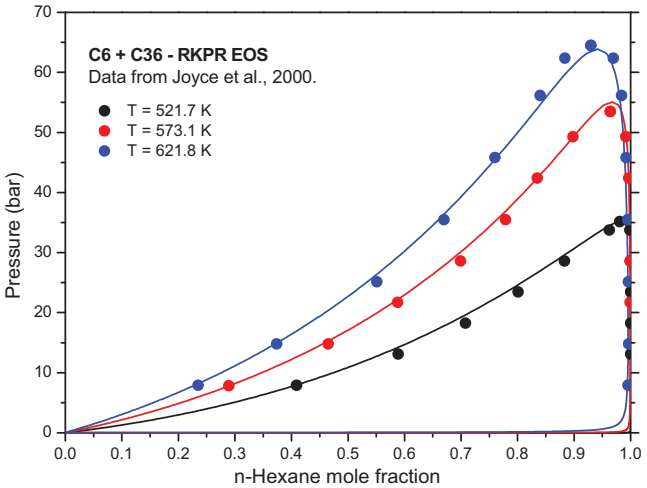

Fig. 20. Prediction of isothermal Pxy diagrams for the systems $C_6 + C_{24}$ and $C_6 + C_{36}$, with the RKPR EOS and correlations developed in this work. Experimental data from [34].

critical region at three different temperatures, published by Nieuwoudt [31] (Fig. 18). In both cases the predictions based on the new correlations for the l_{ij} parameter (Eqs. (11)–(12) and constants from Table 4) and null k_{ij}, provide a very satisfactory representation of the data. The high pressure VLE behavior in mixtures of *n*-hexane also seems to be properly captured by the proposed correlations, as it can be seen from the prediction of critical lines in Fig. 19 and Pxy diagrams for the more asymmetric systems with data available: $C_6 + C_{24}$ and $C_6 + C_{36}$ in Fig. 20 and also $C_6 + C_{16}$ in Fig. B9 (Supplementary material).

3. Conclusions

Based on successful results of a previous publication which focused on different methane and ethane + *n*-alkane binary systems individually parameterized, in this work a new parameterization of the RKPR EoS was developed and presented for *n*-alkanes. It includes binary interactions but also pure compound parameters, based on the structural δ_1 parameter as a function of the alkane carbon number, besides the classical matching of critical temperature, pressure and acentric factor.

With the new pure compound parameters table, and correlating the l_{ij} repulsive parameter with the δ_1 value for the heavier alkane, the use of attractive interaction parameters (k_{ij}) was only necessary for the methane and also the more asymmetric part of the propane series.

Results for the methane and ethane series of binaries, in the widest possible ranges of temperature, pressure, composition and asymmetry, have in average the same quality as those presented in the previous work, with the advantage that the new correlations allow for making predictions for any system, and those predictions have been shown to be very accurate when compared to high quality data which had not been at all considered for the development of the correlations. For the propane and –with less data available- also higher series, the proposed correlations also provided very good predictions for both critical lines and subcritical VLE behavior.

Overall, based on the presented results for binary systems, the RKPR with this new parameterization of both pure compound and interactions for *n*-alkanes, appears as a promising model for describing the phase behavior of hydrocarbon mixtures, especially when asymmetry is present and the classic cubic equations like SRK and PR fail. Indeed, results for ternary and synthetic multicomponent fluids indicate a very good predictive capacity of the correlations developed in this work, and its potential for use in oil and gas thermodynamic modeling and PVT simulation. Those results will be part of another article, currently in preparation.

At the same time, and from a more basic perspective, the successful results of the proposed predictive correlations for the RKPR EoS have shown that is not necessary to resort to the complexity of for example SAFT type models to accurately capture the phase behavior of the more asymmetric hydrocarbon mixtures. In other words, the limitations encountered in classic models like SRK and PR were not because of their cubic nature but rather because of their two-parameter structure implying for example universal critical compressibility factors among other things. The way in which the third parameter δ_1 breaks such rigidity in the structure of the cubic equation of state for the RKPR EoS (in a way, analogous to what the *m* parameter does in SAFT type equations) has now proven to be appropriate enough to capture the complex phase behaviors of the more asymmetric hydrocarbon mixtures. Comparable results providing predictive capacity based on SAFT or related models are so far, to the best of our knowledge, not available in the literature.

Acknowledgements

We acknowledge the financial support received from the following Argentinean institutions: Consejo Nacional de Investigaciones Científicas y Técnicas de la República Argentina (CONICET)>, Agencia Nacional de Promoción Científica y Tecnológica (ANPCyT), Secretaría de Políticas Universitarias (SPU) and Universidad Nacional de Córdoba (UNC).

Appendix A. Supplementary data

Supplementary data associated with this article can be found, in the online version, at http://dx.doi.org/10.1016/j.fluid.2015.06.005.

References

[1] M. Cismondi Duarte, M.V. Galdo, M.J. Gomez, N.G. Tassin, M. Yanes, High pressure phase behavior modeling of asymmetric alkane+alkane binary systems with the RKPR EOS, Fluid Phase Equilib. 362 (2014) 125–135, doi: http://dx.doi.org/10.1016/j.fluid.2013.09.039.
[2] M. Cismondi, J. Mollerup, Development and application of a three-parameter RK-PR equation of state, Fluid Phase Equilib. 232 (2005) 74–89.
[3] K.S. Pedersen, P.L. Christensen, Phase Behavior of Petroleum Reservoir Fluids, CRC/Taylor & Francis, 2006.
[4] J.N. Jaubert, F. Mutelet, VLE predictions with the Peng–Robinson equation of state and temperature dependent k_{ij} calculated through a group contribution method, Fluid Phase Equilib. 224 (2004) 285–304, doi:http://dx.doi.org/10.1016/j.fluid.2004.06.059.
[5] P. Marteau, P. Tobaly, V. Ruffier-Meray, J.C. De Hemptinne, High-pressure phase diagrams of methane + squalane and methane + hexatriacontane mixtures, J. Chem. Eng. Data 43 (1998) 362–366.
[6] J. Jaubert, R. Privat, F. Mutelet, Predicting the phase equilibria of synthetic petroleum fluids with the PPR78 approach, AIChE J. 56 (2010) 3225–3235.
[7] H.J. van der Kooi, E. Flöter, T.W. d Loos, High-pressure phase equilibria of $\{(1-x)CH_4 + xCH_3(CH_2)\ 18CH_3\}$, J. Chem. Thermodyn. 27 (1995) 847–861.
[8] E. Flöter, T.W. De Loos, J. De Swaan Arons, High pressure solid–fluid and vapour–liquid equilibria in the system (methane + tetracosane), Fluid Phase Equilib. 127 (1997) 129–146.
[9] J.J.B. Machado, T.W. De Loos, Liquid–vapour and solid–fluid equilibria for the system methane + triacontane at high temperature and high pressure, Fluid Phase Equilib. 222–223 (2004) 261–267.
[10] E.C. Voutsas, G.D. Pappa, K. Magoulas, D.P. Tassios, Vapor–liquid equilibrium modeling of alkane systems with Equations of State: simplicity versus complexity, Fluid Phase Equilib. 240 (2006) 127–139.
[11] A. Tihic, G.M. Kontogeorgis, N. von Solms, M.L. Michelsen, Applications of the simplified perturbed-chain SAFT equation of state using an extended parameter table, Fluid Phase Equilib. 248 (2006) 29–43.
[12] C. McCabe, A. Galindo, M.N. García-Lisbona, G. Jackson, Examining the adsorption (vapor–liquid equilibria) of short-chain hydrocarbons in low-density polyethylene with the SAFT-VR approach, Ind. Eng. Chem. Res. 40 (2001) 3835–3842, doi:http://dx.doi.org/10.1021/ie0101386.
[13] D. Ambrose, C. Tsonopoulos, Vapor–liquid critical properties of elements and compounds. 2. Normal alkanes, J. Chem. Eng. Data 40 (1995) 531–546.
[14] C.E. Schwarz, I. Nieuwoudt, Phase equilibrium of propane and alkanes part II: hexatriacontane through hexacontane, J. Supercrit. Fluids. 27 (2003) 145–156.
[15] M. Cismondi, M.E. Gaitán, GPEC (Global Phase Equilibrium Calculations) 2013. http://gpec.phasety.com/.
[16] M. Cismondi, M.L. Michelsen, M.S. Zabaloy, Automated generation of phase diagrams for supercritical fluids from equations of state, Proceedings of the 11th European Meeting on Supercritical Fluids, Barcelona-Spain, 2008.
[17] M. Cismondi, M. Michelsen, Automated calculation of complete Pxy and Txy diagrams for binary systems, Fluid Phase Equilib. 259 (2007) 228–234.
[18] M. Cismondi, M.L. Michelsen, Global phase equilibrium calculations: critical lines, critical end points and liquid–liquid–vapour equilibrium in binary mixtures, J. Supercrit. Fluids 39 (2007) 287–295.
[19] M. Cismondi, M.L. Michelsen, M.S. Zabaloy, Automated generation of phase diagrams for binary systems with azeotropic behavior, Ind. Eng. Chem. Res. 47 (2008) 9728–9743.
[20] J. Pauly, J. Coutinho, J.L. Daridon, High pressure phase equilibria in methane + waxy systems. 1. Methane + heptadecane, Fluid Phase Equilib. 255 (2007) 193–199.
[21] W.L. Weng, M.J. Lee, Vapor–liquid equilibrium of the octane/carbon dioxide, octane/ethane, and octane/ethylene systems, J. Chem. Eng. Data 37 (1992) 213–215, doi:http://dx.doi.org/10.1021/je00006a020.
[22] F.N. Tsai, S.H. Huang, H.M. Lin, K.C. Chao, Solubility of methane ethane, and carbon dioxide in *n*-hexatriacontane, J. Chem. Eng. Data 32 (1987) 467–469.
[23] K.A.M. Gasem, B.A. Bufkin, A.M. Raff, R.L. Robinson, Solubilities of ethane in heavy normal paraffins at pressures to 7.8 MPa and temperatures from 348 to 423K, J. Chem. Eng. Data 34 (1989) 187–191, doi:http://dx.doi.org/10.1021/je00056a012.

[24] C.J. Peters, J. Spiegelaar, J. De Swaan Arons, Phase equilibria in binary mixtures of ethane + docosane and molar volumes of liquid docosane, Fluid Phase Equilib. 41 (1988) 245–256.
[25] C.J. Peters, R.N. Lichtenthaler, J. de Swaan Arons, Three phase equilibria in binary mixtures of ethane and higher *n*-alkanes, Fluid Phase Equilib. 29 (1986) 495–504.
[26] C.E. Schwarz, I. Nieuwoudt, Phase equilibrium of propane and alkanes part I. Experimental procedures, dotriacontane equilibrium and EOS modelling, J. Supercrit. Fluids 27 (2003) 133–144.
[27] H.H. Reamer, B.H. Sage, Phase equilibria in hydrocarbon systems: volumetric and phase behavior of the propane-*n*-decane system, J. Chem. Eng. Data 11 (1966) 17–24.
[28] J. Gregorowicz, T.W. De Loos, J. De Swaan Arons, The system propane + eicosane: P, T, and *x* measurements in the temperature range 288–358 K, J. Chem. Eng. Data 37 (1992) 356–358.
[29] C.J. Peters, J.L. de Roo, J. de Swaan Arons, Phase equilibria in binary mixtures of propane and hexacontane, Fluid Phase Equilib. 85 (1993) 301–312.
[30] V.V. de Leeuw, T.W. de Loos, H.A. Kooijman, J. de Swaan Arons, The experimental determination and modelling of VLE for binary subsystems of the quaterhary system $N_2 + CH_4 + C_4H_{10} + C_{14}H_{30}$ up to 1000 and 440 K, Fluid Phase Equilib. 73 (1992) 285–321.
[31] I. Nieuwoudt, Vapor–liquid equilibria and densities for the system butane + hexacontane, J. Chem. Eng. Data (1996) 1024–1027.
[32] P.C. Joyce, M.C. Thies, Vapor–liquid equilibria for the hexane + hexadecane and hexane + 1-hexadecanol systems at elevated temperatures and pressures, J. Chem. Eng. Data (1998) 819–822, doi:http://dx.doi.org/10.1021/je980037n.
[33] C.P. Hicks, C.L. Young, The gas–liquid critical properties of binary mixtures, Chem. Rev. 75 (1975) 119–175.
[34] P.C. Joyce, J. Gordon, M.C. Thies, Vapor–liquid equilibria for the hexane + tetracosane and hexane + hexatriacontane systems at elevated temperatures and pressures, J. Chem. Eng. Data 45 (2000) 424–427, doi: http://dx.doi.org/10.1021/je990229y.
[35] C. Tsonopoulos, Z. Tan, The critical constants of normal alkanes from methane to polyethylene, Fluid Phase Equilib. 83 (1993) 127–138, doi:http://dx.doi.org/10.1016/0378-3812(93)87015-S.
[36] K. Magoulas, D.P. Tassios, Thermophysical properties of *n*-alkanes from C1 to C_{20} and their prediction for higher ones, Fluid Phase Equilib. 56 (1990) 119–140.